

TIME-DEPENDENT SIMULATION OF CHARGE TRANSFER IN SURFACE-CHANNEL CHARGE-COUPLED DEVICES

G. B. Tripodi*, P. Ciampolini, M. Rudan and G. Baccarani

Dipartimento di Elettronica, Università di Bologna
viale Risorgimento 2, 40136 Bologna, Italy

*Istituto per la Ricerca Scientifica e Tecnologica
Pantè di Povo, 38050 Trento, Italy

1. Introduction

Charge transfer in charge-coupled devices (CCD's) has been thoroughly investigated in the seventies [1-11] due to the need of achieving extremely-low transfer inefficiencies ($\epsilon \simeq 10^{-5}$) for both signal processing and imaging applications. Due to the difficulty of a complete numerical simulation, however, analytical models based on a number of simplifying assumptions and tailored to a specific device geometry were developed [2-5]. These models led to a qualitative understanding of the physical mechanisms affecting the transfer inefficiency, but a quantitative and realistic analysis of charge transfer in CCD's has not been attempted.

In the previously-mentioned models, the inherent coupling between the transport process and the potential distribution has been overcome by a rather artificial distinction between the self-induced electric field and the fringing field. The former is due to the non-uniform lateral distribution of the mobile charge, while the latter is due to the device geometry and applied biases in the absence of charge packets. Due to the approximately-linear relationship between the surface potential and the stored charge, the self-induced field generates a current term proportional to the gradient of the charge itself: thus, charge transfer is viewed as a modified diffusion process occurring within a fixed fringing field.

The field configuration in surface-channel CCD's has been typically determined by means of a Fourier-series expansion of the electric potential [10,11] within the device unit-cell; this method, however, is based on a number of simplifying assumptions: *i*) the depletion width is assumed to be uniform; *ii*) the charge at the Si-SiO₂ interface is strictly two-dimensional (charge-sheet model) and, *iii*) the lateral distribution of the mobile charge is not determined self-consistently, but it is arbitrarily set to a constant value. Alternatively, numerical integration of Poisson's equation within the unit-cell of the CCD has been performed in static conditions by neglecting the mobile charge at the interface [6-9], in order to determine the fringing field acting upon the carriers during the transfer process.

Incomplete charge transfer occurs in CCD's due to the finite time allowed by the clock waveforms: especially during the latest stage of transfer, when

both diffusion and self-induced field become scarcely effective, the key role is played by the fringing field. It is therefore necessary that the latter penetrates deeply underneath the storage electrode, so that carriers cannot long reside in the original well but, rather, are quickly swept across it and transferred to the new charge location. An additional cause for transfer inefficiency is due to charge trapping at interface states: carriers get trapped during the storage of the charge packet in view of the locally-large carrier concentration at the surface. During the transfer process, trapped carriers are re-emitted with time constants related to the energy level of the trapping state. For deep levels, this time constant may be as long as 10^{-2} sec., i.e. far larger than the transfer time. In most cases these charges will be re-emitted during the following clock cycles, thus contributing to the device transfer inefficiency.

In this paper we discuss a time-dependent simulation of charge transfer in a 2-phase surface-channel CCD, which has been performed using HFIELDS. In order to make the program suitable for such a task, periodic boundary conditions have been incorporated into the code, thus allowing for the simulation of strictly one CCD cell without unnecessary extensions of the device cross section.

In principle, the trapping-detrapping mechanism requires an additional continuity equation for the trapped charge to be solved. So far, this has not been implemented in HFIELDS. Therefore, we assume an energy-distributed interface-state density and use the SRH generation-recombination rate strictly valid in DC conditions [12]. We expect this procedure to provide quantitatively good results for small interface-state densities, compared with the density of charge being transferred.

2. Numerical techniques

In order to efficiently simulate the charge-transfer process in a CCD, periodic boundary conditions (B.C.) must be used at the left and right boundaries of the unit cell. Thus we have

$$\varphi(0, y) = \varphi(L, y) \quad (1, a)$$

$$n(0, y) = n(L, y) \quad (1, b)$$

$$p(0, y) = p(L, y) \quad (1, c)$$

$$D_x(0, y) = D_x(L, y) \quad (2, a)$$

$$J_{nx}(0, y) = J_{nx}(L, y) \quad (2, b)$$

$$J_{px}(0, y) = J_{px}(L, y) \quad (2, c)$$

where the symbols are given their usual meaning, and L is the length of the unit cell. At the boundaries $x = 0$ and $x = L$, indeed, the Neumann B.C. cannot be applied, for the normal components of both currents and field cannot be taken as being vanishingly small.

From a practical standpoint, imposing periodic B.C. within a general-purpose device simulator implies a number of consistency checks, in order to

make sure that not only the device geometry, but also the discretization mesh, can be extended with a periodicity law without discontinuities at the boundary of the cell. More specifically, for every mesh point at the left boundary, a corresponding one with the same vertical coordinate and the same qualification (semiconductor, insulator, contact, gate, interface, etc.) must exist at the right boundary.

In order to ensure that periodic boundary conditions are indeed fulfilled, during the assembly of the Jacobian matrix the couples of nodes related by the periodicity condition are effectively treated as being one single node, as if they were geometrically coincident.

The details of the time-dependent solution algorithm are reported in [13]. Here it may suffice to say that the transient analysis is performed by HFIELDS using a simple first-order backward difference formulation of the device equations (backward Euler). This method is known to be both A- and L-stable, but must be supplemented by a proper automatic definition of the time step, so that the local truncation error is kept under control.

The latter is defined as

$$LTE = \left| \frac{d^2(\varphi - \varphi_{n,p})}{dt^2} \right| \frac{(\Delta t_k)^2}{2V_{th}} \quad (3, a)$$

which, in discretized form, becomes

$$(LTE)_k = \left| [h_{k+1}(\varphi - \varphi_{n,p})_{k+1} - 2h_k(\varphi - \varphi_{n,p})_k + h_{k-1}(\varphi - \varphi_{n,p})_{k-1}] \right| \frac{(\Delta t_k)^2}{(2V_{th})} \quad (3, b)$$

where V_{th} is the thermal voltage and

$$h_{k+1}^{-1} = \Delta t_{k+1}(\Delta t_{k+1} + \Delta t_k)/2 \quad (4, a)$$

$$h_k^{-1} = \Delta t_{k+1}\Delta t_k \quad (4, b)$$

$$h_{k-1}^{-1} = \Delta t_k(\Delta t_{k+1} + \Delta t_k)/2. \quad (4, c)$$

Unfortunately, $(\varphi - \varphi_{n,p})_{k+1}$ is still unknown at the k^{th} time step, so that $(LTE)_{k-1}$ rather than $(LTE)_k$ is numerically computed. Next, the new candidate time step Δt_{k+1}^* is determined according to the expression

$$\Delta t_{k+1}^* = \Delta t_k \left[\frac{c_t}{|(LTE)_{k-1}|_{max}} \right]^{1/2} \quad (5)$$

where c_t is the admitted truncation error and $|(LTE)_{k-1}|_{max}$ is the maximum value of the LTE's. If $\Delta t_{k+1}^* < \Delta t_k$, the previous time step is rejected and a new computation is started with $\Delta t_k = \omega \Delta t_{k+1}^*$, where ω is an adjustable parameter smaller than 1. Otherwise, the previous solution is accepted and $\Delta t_{k+1} = \min[\Delta t_k(1 - \omega) + \Delta t_{k+1}^*\omega, 2\Delta t_k]$. The last rule restricts the timestep rate of increase, and is intended to avoid step-size oscillations.

3. Results

The discretization mesh of the simulated structure is shown in figure 1. The latter is a 24 μm long, 4-electrode CCD cell with the origin set at the middle of a storage electrode. The oxide thicknesses under the storage and transfer gates are 100 nm and 300 nm, respectively. Also, the threshold voltage under the transfer electrodes is adjusted to an intermediate value between the high and low values of the clocking voltages by a suitable channel implant. So doing, the maximum charge handling capability (and dynamic range) compatible with a 2-phase clocking scheme is obtained.

The latter is illustrated in figure 2. For $t < 0$, ϕ_1 is set at a low value (≈ 0.5 V), just below the device threshold under the storage gate; ϕ_2 is set instead at 2.5 V so that an inversion layer is well developed under the storage electrode at the initial condition. ϕ_2 is then raised to 5.5 V in order to achieve a non-equilibrium condition with a signal charge equal to nearly 80% of the maximum charge-handling capability. At the time $t = 0$, ϕ_1 is raised to 5.5 V with a raise time of 20 nsec, in order to allow the charge transfer to occur. At the time $t = 40$ nsec, ϕ_2 starts dropping to the low value, which is reached after 300 nsec. Finally 40 nsec are additionally left to allow the transfer process to be completed.

Figure 3 shows a perspective plot of the electric potential within the simulated structure at the time $t = 0$. The higher threshold voltage below the transfer gates strongly depresses the corresponding surface potential, also plotted in figure 4, thereby isolating the charge packet below the central electrode. The dip of the surface potential between the transfer gate and the empty storage gate is due to the lateral penetration of the channel implant. The electron distribution is shown in figure 5. It should be noticed that the vertical log-scale does not emphasize the difference in carrier concentration at the storage electrodes: a linear plot of the latter at the Si-SiO₂ interface, shown in figure 6, provides a more realistic view of the relative amount of the two charge packets. Nevertheless, an even smaller charge at the supposedly-empty storage electrode, i.e. a smaller DC bias and/or a larger threshold voltage would have been desirable.

The electric potential at the time $t = 20$ nsec., i.e. at the beginning of the transfer process, is shown in figure 7. The different values of the surface potential at the two storage electrodes, and therefore the different voltage drops across the oxide, reflect again the difference in space charges per unit area. The corresponding electron concentration is illustrated in figure 8, and shows that little changes have occurred in the mobile charge distribution. The electric potential at the time $t = 340$ nsec. is shown in figure 9, where the initial condition is nearly reversed between the two storage and transfer electrodes.

Figure 10 shows a plot of the integrated charge below the two storage electrodes against time. The transfer process occurs in a nearly-linear fashion during the fall time of ϕ_2 , but it is slowed down during the latest part of the transfer. The sum of the two curves represents the total amount of charge initially stored within the CCD cell. It turns out to be constant within 1%, indicating that the discretization error associated with the time-dependent simulation, using a linear interpolation scheme (backward Euler) and an au-

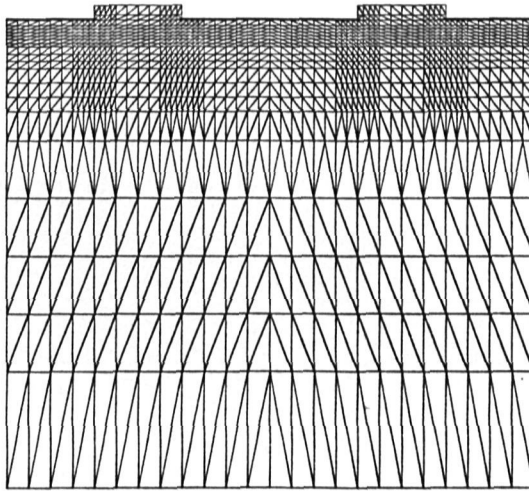


Figure 1: Mesh of the simulated CCD.

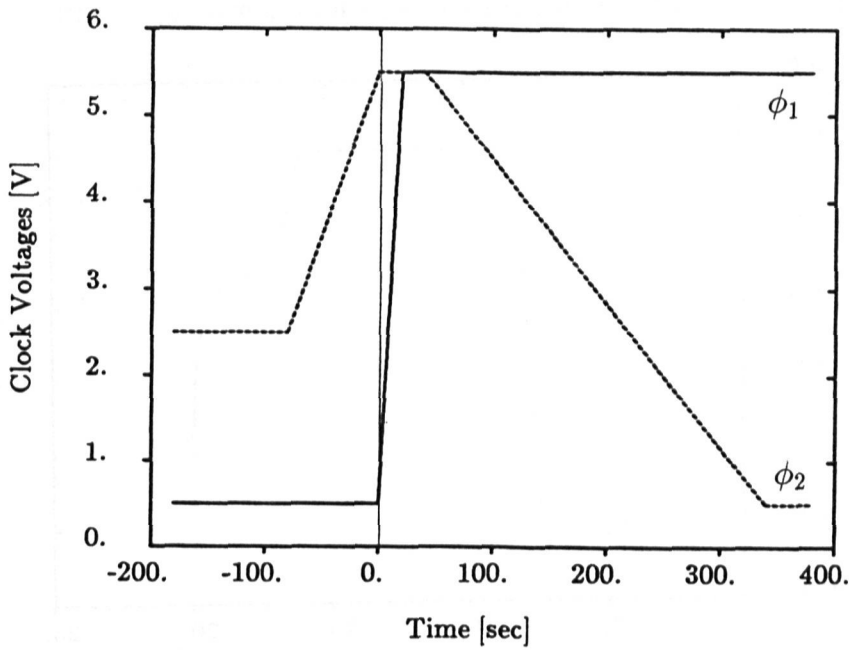


Figure 2: Clocking scheme.

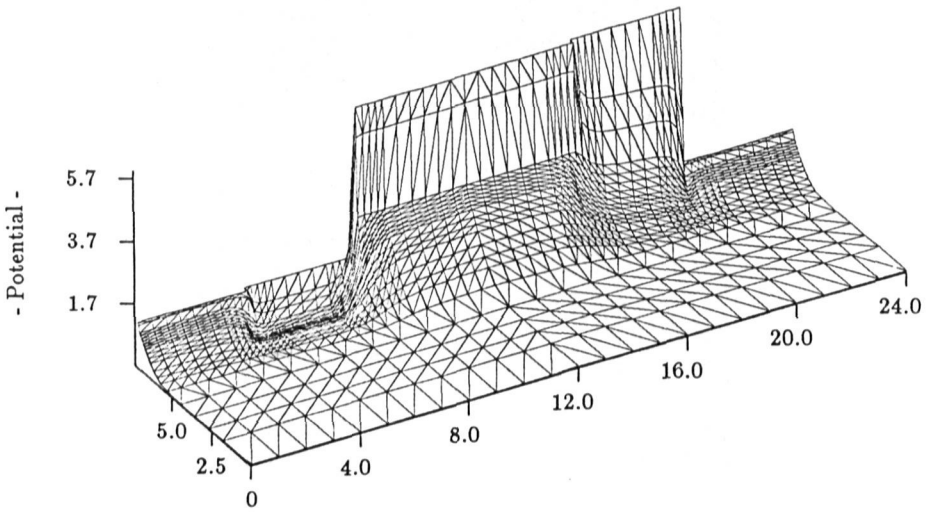


Figure 3: Electric potential at the time $t = 0$ ($\phi_1 = 0.5\text{V}$, $\phi_2 = 5.5\text{V}$).

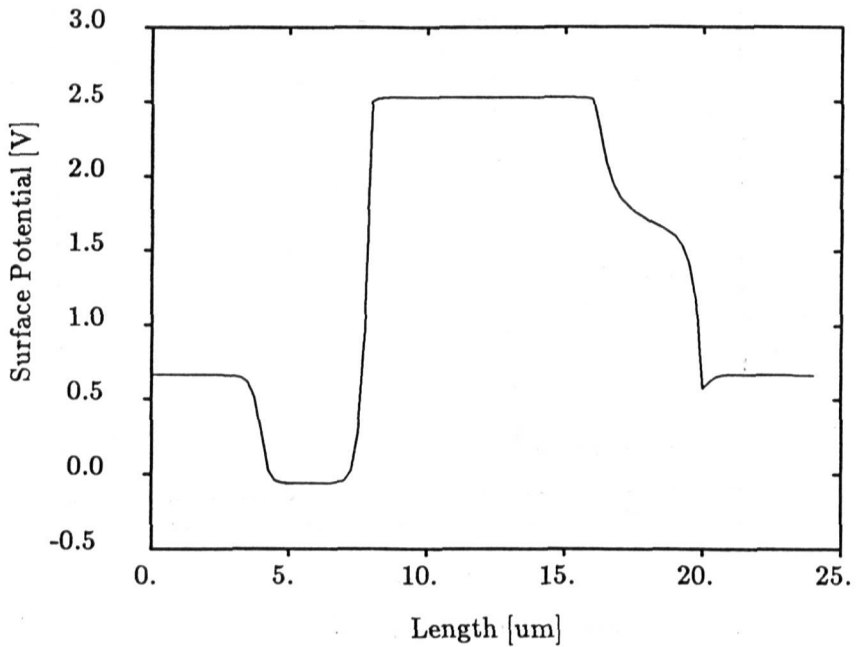


Figure 4: Surface potential at the time $t = 0$.

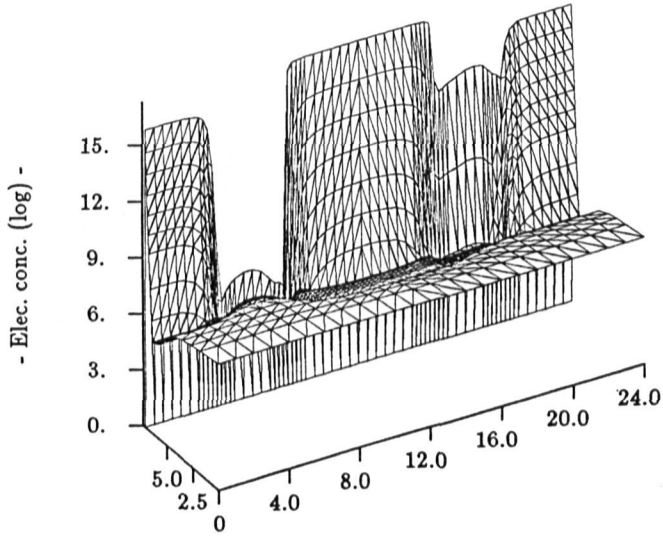


Figure 5: *Electron concentration at the time $t = 0$.*

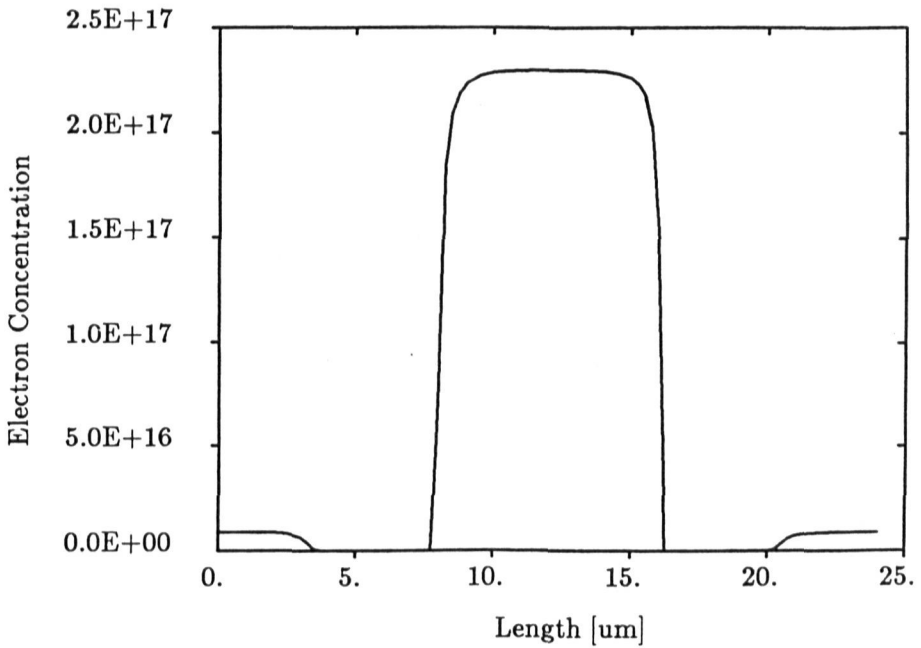


Figure 6: *Surface electron concentration at the time $t = 0$.*

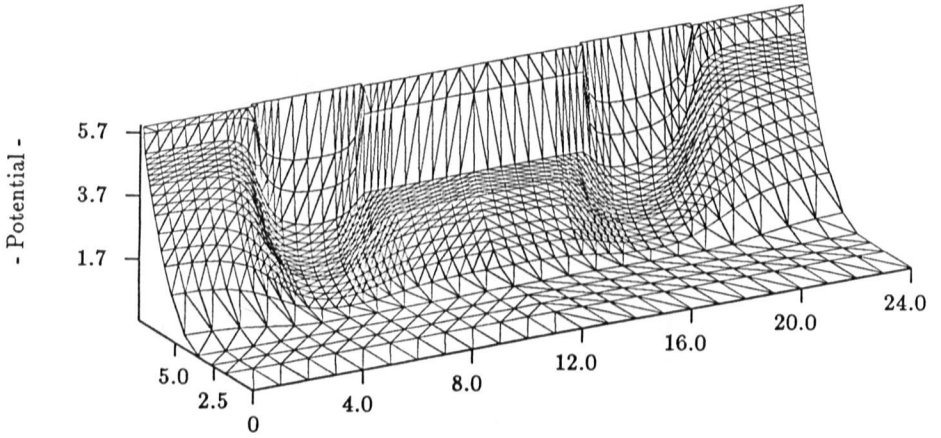


Figure 7: Electric potential at the time $t = 20$ nsec ($\phi_1 = 5.5$ V, $\phi_2 = 5.5$ V).

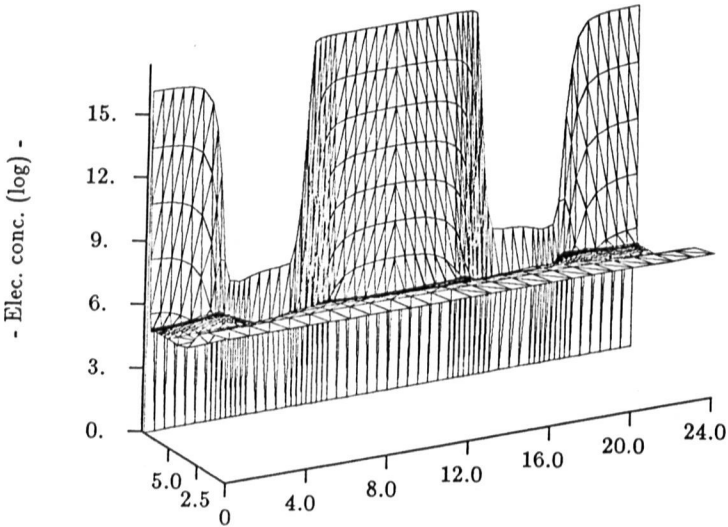


Figure 8: Electron Concentration at the time $t = 20$ nsec.

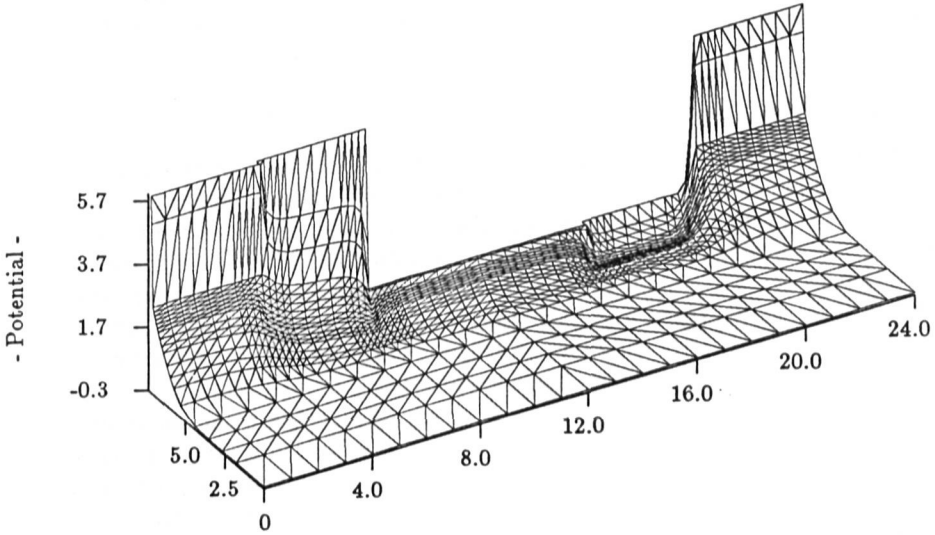


Figure 9: *Electric potential at the time $t = 340$ nsec ($\phi_1 = 5.5V$, $\phi_2 = 0.5V$).*

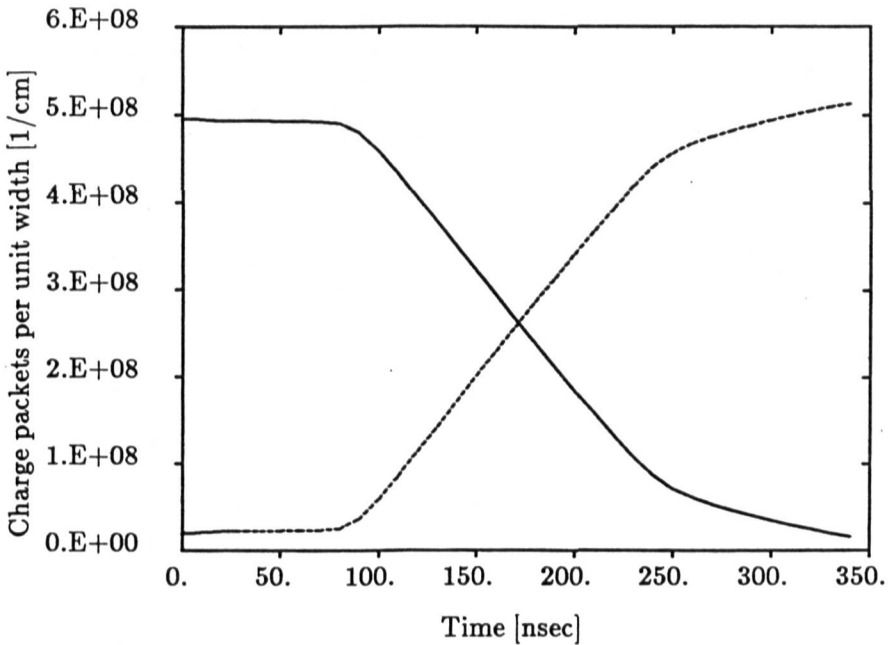


Figure 10: *Charge packets (per unit width) against time at the initial and final storage electrodes.*

omatic definition of the time step, is about of the same order. Thus, the resulting value of the transfer inefficiency may be subject to a relatively-large error. An improved accuracy could be achieved by either using a higher-order formulation of the time-dependent discretization scheme or, at the expense of a longer CPU time, by imposing a smaller truncation error.

4. Conclusions

In this work we have examined the detailed behaviour of the transfer process within the unit-cell of a surface CCD. The simulations have been carried out in dynamic conditions using a general-purpose device simulator (HIELDS) allowing for periodic boundary conditions. Trapping-detrapping effects have been accounted for in a simplified way by assuming energy-distributed interface states at the Si-SiO₂ interface in connection with capture and emission rates strictly valid only in DC. So doing, an additional continuity equation for the trapped carriers has been avoided.

The program employs a first-order backward-Euler discretization scheme of the semiconductor equations with a proper automatic definition of the time step which is intended to keep the local truncation error below a predefined amount ϵ_t while, at the same time, avoiding unnecessary computations.

In this example, numerical simulation has turned out to be a useful design tool: electric potential and field, carrier concentrations and charge densities per unit area can be self-consistently determined without unnecessary simplifying assumptions. Thus, the CCD dynamic range can be suitably optimized by a proper selection of the clock waveforms and of the channel implant below the transfer gates. A quantitative prediction of the transfer inefficiency against frequency, however, turns out to be a difficult task in view of the extremely small values of ϵ , which are usually below the practical range of the error associated with the time-dependent discretization scheme.

Acknowledgements

This work has been partially supported by the National Research Council (CNR) under "Progetto Finalizzato MADESS". Support from SGS-Thomson is also gratefully acknowledged.

References

- [1] C. H. Séquin, M. F. Tompsett: "Charge transfer devices", Academic Press, New-York, 1975.
- [2] W. E. Engeler, J. J. Tiemann, R. D. Baertsch: "Surface Charge Transport in a Multielement Charge Transfer Structure", *Jour. of Appl. Physics*, vol. 43, pp. 2277-2285, 1972.
- [3] J. E. Carnes, W. F. Kosonocky, E. G. Ramberg: "Free Charge Transfer in Charge Coupled Devices", *IEEE Trans. on Electron Devices*, vol. ED-19, pp. 798-808, 1972.
- [4] L. G. Heller, H. S. Lee: "Digital Signal Transfer in Charge Transfer Devices", *IEEE Jour. of Solid-State Circuits*, vol. SC-8, pp. 116-125, 1973.

- [5] C. N. Berglund, K. K. Thornber: "Incomplete Transfer in Charge Transfer Devices", *IEEE Jour. of Solid-State Circuits*, vol. SC-8, pp. 108-116, 1973.
- [6] J. E. Carnes, W. F. Kosonocky, E. G. Ramberg: "Drift-Aiding Fringing Field in Charge Coupled Devices", *IEEE Jour. of Solid-State Circuits*, vol. SC-6, pp. 322-326, 1971.
- [7] R. J. Strain, N. L. Schryer: "A Non-Linear Diffusion Analysis of Charge Coupled Device Transfer", *Bell Syst. Tech. Jour.*, vol. 50, pp. 1721-1740, 1971.
- [8] G. F. Amelio: "Computer Modelling of Charge Coupled Device Characteristics", *Bell Syst. Tech. Jour.*, vol. 51, pp. 705-730, 1972.
- [9] L. G. Heller, W. H. Chang, W. A. Lo: "A model of Charge Transfer in Bucket Brigade and Charge Coupled Devices", *IBM Jour. of Res. and Dev.*, vol. 16, pp. 184-187, 1972.
- [10] J. Mc Kenna, N. L. Schryer: "The Potential in a Charge Coupled Device with no Mobile Minority Carriers", *Bell Syst. Tech. Jour.*, vol. 52, pp. 669-696, 1973.
- [11] G. Baccarani, A. M. Mazzone, M. Rudan: "Electric Potential and Field in Surface-Channel Charge-Coupled Devices", *Alta Frequenza*, vol. 45, pp. 291-294, 1976.
- [12] A. Gnudi, P. Ciampolini, R. Guerrieri, M. Rudan, G. Baccarani: "Small-Signal Analysis of Semiconductor Devices Containing Generation-Recombination Centers", *Proceedings of the Fifth International Conference on the Numerical Analysis of Semiconductor Devices and Integrated Circuits (NASECODE V)*, pp. 207-212, Boole Press, Dublin, 17-19 June, 1987.
- [13] R. Guerrieri, P. Ciampolini, A. Gnudi, M. Rudan, G. Baccarani: "Time-dependent simulation of a dynamic RAM cell", *Proc. of the First International Conference on Computer Technology (COMP EURO 87)*, pp. 333-336, Hamburg, Germany, May 11-15, 1987.